2018

PHOTOLUMINESCENCE FROM GAN CO-DOPED WITH C AND SI

Mykhailo Vorobiov
Virginia Commonwealth University

PHOTOLUMINESCENCE FROM GAN CO-DOPED WITH C AND SI

A Thesis submitted in partial fulfillment of the requirements for the degree of Master of Science at Virginia Commonwealth University.

by

MYKHAILO VOROBIOV

B.S. in Electrical Engineering, Kharkiv National University of Radioelectronics, 2013

M.S. in Electrical Engineering, Kharkiv National University of Radioelectronics, 2014

Director: **Michael Reshchikov**,

Professor, Department of Physics

Virginia Commonwewalth University

Richmond, Virginia

May, 2018

Acknowledgements

Thanks to everyone who made this research possible.

TABLE OF CONTENTS

Chapter Page

LIST OF TABLES

LIST OF FIGURES

Abstract

PHOTOLUMINESCENCE FROM GAN CO-DOPED WITH C AND SI

By **Mykhailo Vorobiov**

A Thesis submitted in partial fulfillment of the requirements for the degree of Master of Science at Virginia Commonwealth University.

Virginia Commonwealth University, 2018.

Director: **Michael Reshchikov**,

Professor, Department of Physics

This thesis devoted to the experimental studies of yellow and blue luminescence (YL and BL relatively) bands in Gallium Nitride samples doped with C and Si. The band BL_C was at first observed in the steady-state photoluminescence spectrum under high excitation intensities and discerned from BL1 and BL2 bands appearing in the same region of the spectrum. Using the time-resolved photoluminescence spectrum, we were able to determine the shape of the BL_C and its position at 2.87 eV. Internal quantum efficiency of the YL band was estimated to be 90%. The hole capture coefficient of the BL_C related state was determined as 7×10^{-10} cm^3/s. Properties of BL_C were investigated. The YL and BL_C bands are attributed to electron transitions via the (0/-) and (+/0) transition levels of the C_N defect.

CHAPTER 1

INTRODUCTION

1.1 Gallium Nitride. Properties and importance for industry

Gallium nitride (GaN) is an important semiconductor widely used in electronics industry for years. Current commercial applications of this material primarily include production of blue/green light emitting diodes and lasers, but GaN is also a promising material for high-power/frequency electronic devices [1].

Despite the fact that GaN has been studied extensively, deep level of understanding still yet to be reached. This especially touches the properties of various impurities and other point defects that occur in the process of growth or introduced intentionally.

Many properties of GaN covered in the literature are still controversial and need to be refined. Moreover, various research groups using different measurement methods frequently report incompatible data introducing even more ambiguity.

This lack of understanding and controversy results in restriction of further progress of enhancing the efficiency of the devices built with GaN technology.

Experimental studies of the defects in GaN are also important for the fundamental research. The acquired data allows theorists to develop computational techniques, that in the nearest future should lead to the development of a more general method that will be able to encompass all the ad hoc approaches used so far.

1.1.1 Chemical Properties

GaN was first synthesised by Johnson et al in 1935 [1]. It is a very stable material with significant hardness that has a Wurtzite crystalline structure (Figure 1). Stability

and hardness made GaN to be a very sutable material for coverings. Its pure form resists cracking that makes it well suited for deposition on sapphire an SiC even having mismatch in lattice constants.

By doping the samples with Si and O, one can get n-type GaN, while Mg doping truns it into p-type [2]. However, Si and Mg impurities significantly change the growth process of GaN, introducing tensile stresses and making it fragile [3].

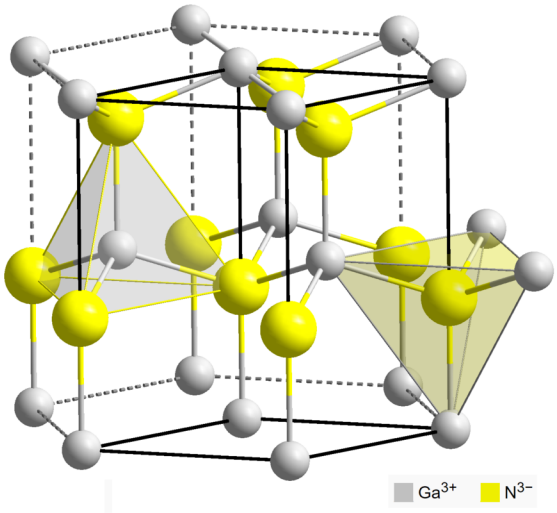

Fig. 1. Crystalline structure of GaN

1.1.2 Electronic Properties

The band structure and the corresponding density of states of GaN calculated using density functional theory (DFT) within local density approximation is depicted in Figure 2. The calculation was performed using GPAW program package with lattice parameters $c = 3.199\ \mathring{A}$ and $c/a = 1.633$. The wavefunctions were represented by 600 plane waves basis states. The calculated bandgap is $E_g = 2.78eV$, which was underestimated compared to the experimental data. However, this calculation reflects the main features of the real

band structure. As one can easily see, GaN is a direct bandgap semiconductor having the conduction band minimum and valence band maximum at the Γ point of the Brillouin zone. The corresponding Brillouin zone is depicted in Figure 3.

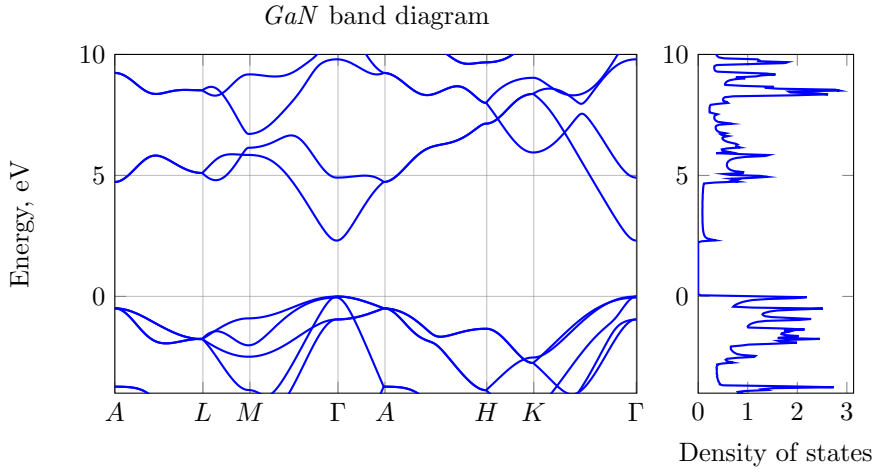

Fig. 2. DFT calculated band structure of GaN

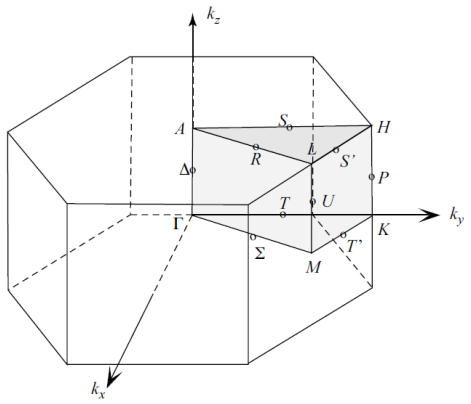

Fig. 3. Brillouin zone and covering scheme of a Wurzite structure

1.2 Shockley-Read-Hall recombination statistics

In 1952 Shockley,Read and Hall [4, 5] developed a phenomenological theory of electron-hole recombination trough trapping mechanism. It was shown experimentally that life-

time of charge carriers strongly depends on the defects and impurities in semiconductors. If a defect introduces an energy level into bandgap, then electron can be captured by the defect. This process is more effective than band-to-band recombination since the transition occurs between energies separated by less than E_g. These impurities are called recombination centers.

Let's consider recombination through a deep defect. Number of defect levels is denoted by N. In order to have recombination via the defects let's assume that only fraction x of them filled with electrons. Hence, the number of defect levels filled with electrons is xN, while the number of unoccupied levels is $(1-x)N$. We can write out the number of caprutes of electrons by the defects in a unit volume per unit of time as

$$R_n = C_n n N(1-x), \tag{1.1}$$

where C_n is the capture coefficient of electrons at the defect level. The rate of thermal emission of electrons from the defect level to the conduction band can be written using the same logic, the only change is that now we need to substitute $N(1-x)$ with Nx and redenote C_n as $\tilde{C}_n$. The result is

$$G_n = \tilde{C}_n N x. \tag{1.2}$$

By the same reasoning, we arrive at the generation rate G_p and capture rate R_p of holes, given by the formulae

$$R_p = C_p p N x \tag{1.3}$$

and

$$G_p = \tilde{C}_p N(1-x). \tag{1.4}$$

The model assumes that the coefficients C_n, $\tilde{C}_n$, C_p and $\tilde{C}_p$ are independent of n, p, N and x. In equilibrium, recombination rate and generation rate of a particular type of carriers

are equal. This condition gives

$$G_n = R_n, \quad G_p = R_P, \tag{1.5}$$

which results in

$$\tilde{C}_n N x = C_n n N (1 - x) \tag{1.6}$$

and

$$\tilde{C}_p N (1 - x) = C_p p N x. \tag{1.7}$$

From the above two relations we get

$$\tilde{C}_n = C_n n \frac{1 - x}{x}, \tag{1.8}$$

$$\tilde{C}_p = C_p p \frac{x}{1 - x}, \tag{1.9}$$

where n, p and x take equilibrium values.

Equilibrium concentration of electrons is given by the formula [6]

$$n_0 = N_c e^{-\frac{E_c - E_F}{k_B T}}, \tag{1.10}$$

where N_c is the density of states in the conduction band, E_c is the energy of the bottom of the conduction band, E_F is the Fermi level and k_B Boltzman's constant. Occupation factor can be chosen to be just Fermi-Dirac distribution

$$x = \frac{1}{g^{-1} e^{\frac{E - E_F}{k_B T}} + 1}, \tag{1.11}$$

where g is degeneracy of the level, E is the energy level of the defect. Substitution of (1.11) into (1.8) and (1.9) allows to eliminate $\tilde{C}_n$ and $\tilde{C}_p$ in further considerations by expressing them through capture coefficients C_n and C_p as

$$\tilde{C}_n = g^{-1} C_n N_c e^{-\frac{E_D}{k_B T}} \tag{1.12}$$

and

$$\tilde{C_p} = g^{-1} C_p N_v e^{-\frac{E_A}{k_B T}}, \tag{1.13}$$

where E_D and E_A are the ionization energies of the defects relative to the condutction and valence bands, respectively. Now, we are in a position to write an effective generation-recombination rate that is

$$G_n - R_n = C_n N \left(n(1-x) - x g^{-1} N_c e^{-\frac{E_D}{k_B T}} \right) \tag{1.14}$$

and

$$G_p - R_p = C_p N \left(px - (1-x) g^{-1} N_v e^{-\frac{E_A}{k_B T}} \right) \tag{1.15}$$

which constitute the core of Shockley-Read-Hall recombination statistics.

In steady regime the rate of electrons captured by the defects is equal to the rate of holes captured by the same type of defect. Hence, two of the above effective rates can be used to solve for x,so that after substiution into either of them, it will result in

$$G_n - R_n = G_p - R_p = \frac{np - n_i^2}{(n + n_1)\tau_p + (p + p_1)\tau_n}, \tag{1.16}$$

where the following notaiton was introduced: n_i is the intrinsic concentration of carriers,

$$n_1 = g^{-1} N_c e^{-\frac{E_D}{k_B T}}, \quad p_1 = g^{-1} N_v e^{-\frac{E_A}{k_B T}}, \tag{1.17}$$

are the concentrations of electrons and holes respectively if in thermodynamic equilibrium the Fermi level coincides with the level of the defect, and

$$\tau_n = \frac{1}{N C_n}, \quad \tau_p = \frac{1}{N C_p} \tag{1.18}$$

are lifetimes of electrons if all the defects were free from electrons, and holes if all the defects were filled with electrons respectively.

1.3 Optical Transitions

In order to better understand the structure of photoluminescence spectra of GaN, let us discuss a number of physical phenomena that contribute to its overall view.

1.3.1 Direct and indirect optical transitions

Before getting to the description of transitions involving impurity states, let's consider probably the most at hand way for non-equilibrium carriers to recombine: band-to-band transitions. This transition occurs primarily in pure materials. Electrons and holes, exited in a sample, tend to accumulate at the extrema of conduction and valence bands respectively, where recombination occurs. If a semiconductor has a direct bandgap (Figure 4), then matrix elements of dipole transitions are non-zero, then electron-hole recombination occurs with high probability. The consequence is that direct bandgap semiconductors, such as GaN, are good radiation emitters. The situation is quite different in

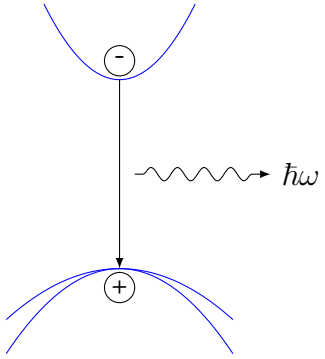

Fig. 4. Direct interband transition scheme

the case of indirect bandgap semiconductors, e.g. Si or GaP. In these materials, in order to happen, transition requires a mediator such as phonon. This condition assures that the conservation laws are not violated. But, according to quantum mechanics, such a three particle process is of low probability. Hence, indirect bandgap semiconductors are usually

bad for optoelectronic applications, especially for high-efficiency light emitters.

1.3.2 Excitonic effects

There are two types of excitons. Frenkel exciton was discovered in 1931 and is the atom excitations that can be transferred from one atom of the material to the other.

For our case it is more important to consider the so-called Wannier-Mott exciton that is a quasi-particle, that represents bound state of a non-equilibrium electron-hole pair. Electron-hole pairs generated in a semiconductor, for example by a laser, can propagate freely through the material. But when they are close enough, so that their Coulomb attraction is significant, then those can be considered as a one hydrogen-like bound state of two particles, that is schematically depicted in Figure 5. If the radius of an exciton is large compared to the lattice constant, then all the formulas for a hydrogen atom can be applied with only slight modification. The essence of the modification is to treat the surrounding material as a continuous medium with permittivity ε that accounts for the screening between two charges.

The above mentioned allows us to write down the excitonic energy levels as

$$E_n = E_g - \frac{\mu \left(\frac{e^2}{4\pi\varepsilon\varepsilon_0}\right)^2}{2\hbar^2} \frac{1}{n^2}, \tag{1.19}$$

where E_g is the bandgap energy, $\mu = \frac{m_e^* m_h^*}{m_e^* + m_h^*}$ is the reduced mass of the electron-hole system with m_e^* and m_h^* being electron and hole effective masses respectively, ε and ε_0 are the relative permittivity of the semiconductor and the permittivity of the vacuum respectively, e is an elementary charge, $\hbar$ is Planck's constants and n is a non-zero positive integer.

These energy levels are typically situated a couple dozens of meV below the bandgap. Therefore, it is typical, at least at low temperature, for transitions to occur through a series

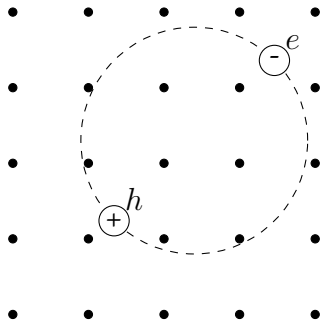

Fig. 5. Wannier-Mott exciton model

of excitonic levels giving rise to a series of peaks below the energy band gap E_g of a particular semiconductor, as in Figure 6, where E_X is the exciton binding energy and E_g is the bandgap.

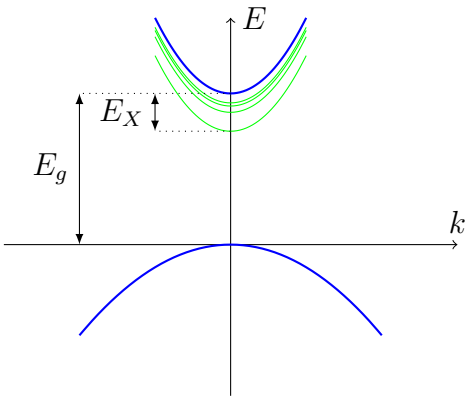

Fig. 6. Exciton levels within energy band scheme of a semiconductor

The intensity of the corresponding peaks depends strongly on temperature. Indeed, since excitonic energies are typically $\sim 10 - 20$ meV, then the exciton-bound electrons can be thermally emitted from these levels to the conduction band. This results in exciton disintegration. Obviously, the higher the temperature, the less probable that electrons and holes will be bound in excitons, resulting in the drop of intensity of the photoluminescence.

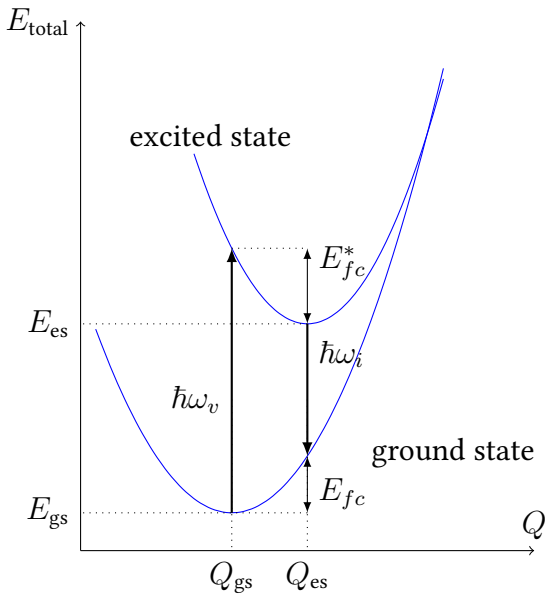

Fig. 7. Configuration coordinate diagram

1.4 Configuration-coordinate model of an optical center

Defect center in a crystal causes significant change in the dispersion law of phonons giving rise to localized vibrational modes. Moreover, the lattice actively takes part in optical transitions since it requires redistribution of electron clouds in the system.

Influenced by a photon, electron on the defect undergoes transition to an excited state, changing its corresponding electron cloud distribution. The lattice responds to this change by relaxation, where surrounding atoms find their new equilibrium positions. Hence, if treated in a simplistic one-dimensional harmonic manner, this can be thought of as the lattice having equilibrium spacing Q_{gs} upon transition establishes new equilibrium atomic spacing Q_{es} as it is depicted in Figure 7.

Now, electron in each of these potentials can be treated as a quantum-mechanical simple harmonic oscillator. In the ground state (of the lattice-electron system), the system oscillates in the potential $\frac{k_{\text{gs}}(Q-Q_{\text{gs}})^2}{2}$, while in the excited state it oscillates in the upper

potential $\frac{k_{es}(Q-Q_{es})^2}{2}$. The corresponding wave functions are well-known

$$\psi_n(Q) = H_n(Q)e^{-\frac{m_e\Omega Q^2}{2\hbar}}, \tag{1.20}$$

where $H_n(Q)$ is a Hermite polynomial of degree n [7]. The corresponding energy levels are given by

$$E_n = \hbar\Omega\left(n + \frac{1}{2}\right), \tag{1.21}$$

where Ω is the characteristic phonon mode frequency and n is a positive integer. According to Frank-Condon principle, in the process of transition, electron cannot affect the motion of the heavy atoms around, they respond to the change post factum, when transition has already happened. Therefore, optical absorbtion and emission can happen only vertically, i.e. for fixed parabolic potentials mentioned above.

It is well known [7] that in coordinate representation the probability to find a particle in any of the vibronic states, except for oscillator's ground state, peaks at the classical turning points. Hence, one can expect that dipole transition matrix elements will be substantially nonzero only from the vibronic ground level of one potential to the edge of the other potential, as it is depicted in Figure 7 for absorbtion process with energy $\hbar\omega_v$ and emission with $\hbar\omega_i$. After electron has undergone transition, lattice relaxes to the corresponding vibronic ground state through emission of phonons. This process obeys usual selection rules for bosonic simple harmonic oscillator, so that hopping takes place only between neighboring vibronic energy levels [8]. Hence, optical transitions begin only from the respective vibronic ground states.

1.5 Non-radiative recombination processes

Not all transitions result in emission of photons. There are certain types of processes that allow a system to release excess of energy without luminescence. These processes

are called non-radiative. Three basic types of such recombinations, classified depending on their final form of their dissipation of energy [8]:

- recombination with transformation of energy into heat through emission of multiple phonons;
- recombination resulting in a creation of a new point defect in the lattice;
- recombination leading to chemical changes in the material.

For our purposes the most useful is to consider the first type.

Multiphonon bimolecular recombination is highly improbable in pure semiconductors, since in wide-bandgap materials a whopping amount of phonons is needed for an electron to recombine with a hole non-radiatively. For example, typical phonon energies are of the order of 50 meV while bandgap of GaN is 3.5 eV, therefore, in order to recombine, electron-hole pair has to emit $\sim$100 phonons. In theory, this process can be described perturbatively, and the described phonon emission will correspond to the very high order expansion term, that is by definition corresponds to negligibly small probability [8].

In the case when a localized luminescence center is present, we can utilize configuration-coordinate model, described in Subsection 1.4. Figure 8 illustrates the multiphonon emission in such a center. The excited center localized around point C can be thermally activated, i.e. surmount point B, with probability

$$p \propto e^{-\frac{E_A}{k_B T}}, \tag{1.22}$$

after which it returns to the ground vibronic state above the point D. In order to reach that point, the center gives off phonons as it is depicted in the figure.

This effect also results in thermal quenching of luminescence. At certain temperature probability to "jump" over the barrier B becomes significant. Hence, assuming that

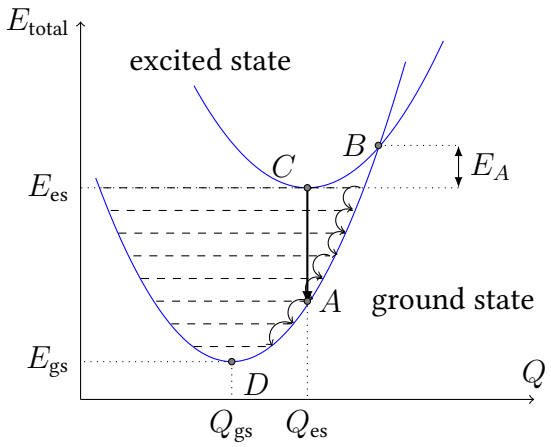

Fig. 8. Multiphonon non-radiative transition in a localized luminescence center

the readiative transition $C \rightarrow A$ is temperature-independent, then the corresponding quantum efficincy is [9, 10]

$$\eta = \frac{1}{1 + \tau_r p_0 e^{-\frac{E_A}{k_B T}}}, \tag{1.23}$$

where τ_r is the radiative lifetime, p_0 is the frequency factor, that takes values of the order of the lattice vibration frequency, E_A is an activation energy of the center.

CHAPTER 2

LITERATURE REVIEW

One of the most notorious defect-induced line in GaN is centered around 2.2-2.3 eV and usually referred to as yellow luminescence (YL). The line is usually observed in n-type GaN regardless of whether the sample is intentionally doped with carbon or not. The nature of the defect related to the line has been discussed for almost thirty years and is still unclear.

The earliest detailed work dedicated to the problem of explaining YL, dates back to 1980 and was carried out by Ogino and Aoki [11]. They investigated GaN samples doped with Si, O and C in order to determine the chemical nature of the impurities causing the YL band. The measurements were carried out in a cryostat at 77 K, and they observed two emission bands: the YL and excitonic. They concluded that doping with C always emphasizes the YL and attributed it to the V_{Ga}-C_{Ga} complex.

In 1995 Van de Walle et al. [12] first adressed the model prposed by Ogino and Aoki. According to their findings V_{Ga}-C_N complex is unstable and tends to dissociate into a V_{Ga} and a C_N acceptor. They proposed that the YL is caused by either V_{Ga} or V_{Ga}-O_N complex. In the theoretical work by Lyons at al. [13] the YL was attributed to the C_N deep acceptor, According to this work, the YL band is caused by optical transitions from the conduction band or a shallow donor level to the $C_N^{0/-}$ level situated at 0.9 eV above the top of the valence band. The corresponding energy of emitted photons is calculated to be 2.14 eV.

However, as it was shown by Demchenko et al. [14] using hybrid functionals technique, the corresponding thermodynamic transition energy of the C_N should be located at 1.09 eV. This number disagrees with experimentally observed 0.85 eV [11] Moreover, if

the YL band was caused by C_N defct, one should also observe a secondart band caused by recombination via the secondary (+/0) transition level related to C_N, as it was suggested by Demchenko et al.

They also suggested that the microscopic mechanism of YL can be explained by the presence of $C_N - O_N$ complex in GaN. Formation energy of the $C_N - O_N$ was calculated to be significantly lower than that of C_N, leading to a suggestion that the concentration of the complexes is sufficient enough to observe strong PL.

The results similar to [13] were reported by Christenson et al. [15]. According to them, unlike in [14], C_N defect has the lowest formation energy, i.e. highly favorable to from. The defect generates PL of 2.18 eV with the corresponding zero-phonon line (ZPL) at 2.67 eV.

In [16] Lyons et al. returned to the problem and refined their calculations. The calculations reproduced the above mentioned result that C_N is a deep acceptor with the energy level $C_N^{0/-}$ at 0.9 eV with PL line at 2.14 eV. However, the authors have found that C_N in GaN exhibits AX-like behavior. In this case, for the Fermi-level close to the valence band maximum the C_N defect can trap a second hole, making C_N^+ charge state stable. The corresponding energy of the (+/0) transition level is 0.35 eV above the valence band maximum. The configuration-coordinate diagram depicted in Figure 9(a) illustrates the optical transition to the (0/-) transition level. The parameters of the transition agree with the previously reported ones in [13] for the process $C_N^0 + e^- \rightarrow C_N^-$. The optical transition scheme depicted in Figure 9(b) describes transitions via the additional (+/0) level. The authors predicted the process $C_N^+ + e^- \rightarrow C_N^0$ that gives rise to the blue emission line at 2.70 eV with the zero-phonon line at 3.15 eV and Frank-Condon shift of 0.45 eV.

The physical consequence of having the charge states C_N^- and C_N^+ is that a GaN sample can emit yellow or blue luminescence lines depending on the position of Fermi-level and the intensity of excitation laser in photoluminescence experiment. In the case of high

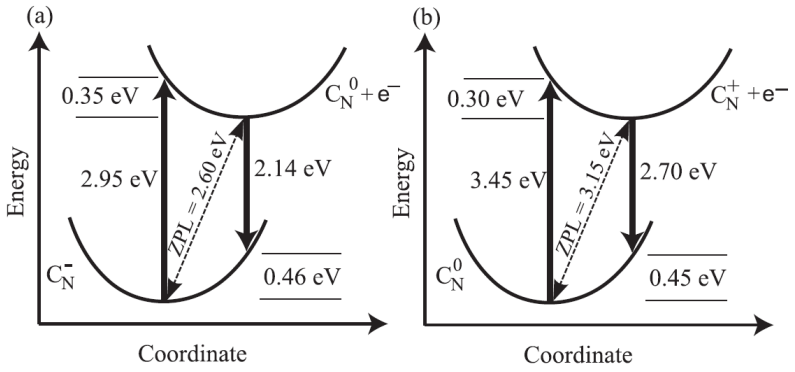

Fig. 9. Configuration-coordinate diagram for C_N defect in GaN (adapted from [16])

excitation intensity this happens when there are enough incident photons capable of ionizing C_N^0 centers in n-type GaN.

Note that early DFT calculations and several experimental studies predicted carbon defect in the nitrogen site C_N to be a shallow acceptor [12]. Despite this fact, C-doped GaN acts in the semi-insulating manner. Lyons proposed that this happens due to self-compensation effect, i.e. incorporation of the C_N acceptor and C_{Ga} donor in equal concentrations.

Plenty of expreimetal attemts were carried out in order to confirm the theoretical suggestions described above and to enhance the previous speculations. However, none of them is conclusive enough and need further clarification.

In [17] luminescence from several GaN samples grown by metal-organic chemical vapor deposition (MOCVD) method and co-doped with C and Si was studied. Along with YL band Seager et al. spotted a blue band at 3 eV in the samples where the concentration of C is greater than Si and the ultra-violet luminescence (UVL) band at 3.3 eV.

GaN samples codoped with Si and C were also studied by Seager et al. in [18]. The samples contained various concentrations of carbon and doped intentionally with silicon. The growth method used was heteroepitaxy on sapphire with MOCVD. The samples in

which concentration of C was greater that that of Si exhibited, beside yellow luminescence, a blue band at 3 eV. The band has a highly non-exponential luminescence decay, that indicates radiative transitions of carriers trapped in a localized state.

In [19] the broad BL band was detected at 2.86 eV in the PL spectrum of GaN samples, grown using molecular beam epitaxy and doped with C. Concentration of C was $\sim 10^{18}$ cm^{-3} both in semi-insulating and n-type material. The authors attributed this band to transtions from C_{Ga} deep donor to C_N acceptor complex.

In [20] YL with maximum at 2.2 eV claimed to be caused by C_NO_N complex, while in high-purity samples one would expect to observe YL related to C_N defect with the maximum at 2.1 eV and accompanying green luminescence (GL) at 2.4 eV. In this study the GL band was observed only in high-purity GaN samples grown by the hydride vapour physical epitaxy (HVPE) method. The transition levels of the C_N were predicted using first-principles calculations to be 1.04 eV for (-/0) level and 0.48 eV for (0/+) level above the valence band maximum.

An exhaustive study of fine structure of the YL in undoped and Si-diped GaN smaples is presented in [21]. The samples were studied by steady-state and time-resolved PL. In this work authors observed ZPL of the YL at 2.57 eV at low exictation intensity and low temperature. At elevated temperatures, ZPL emerged at 2.59 eV that was attributed to the electron transition from a conduction band to the same deep-level defect.The conclusion of the article is that the same defect is responsible for the YL band in undoped GaN frown by HVPE, in undoped GaN grown by MOCVD with carbon as the dominant acceptor, and in Si-doped GaN grown by MOCVD with concentrations.

A very recent characterization of YL band can be found in [10] where varying thermal quenching behavior was observed in various GaN samples. The authors showed that in all samples YL is caused by the same luminescence center and in conductive n-type GaN its ionization energy is determined to be ~ 0.9 eV. The YL was attributed to either C_N or

C_NO_N complex.

Yellow luminescence line has been extensively studied by experimentalists in the effort to establish the defect related to its appearance. Currently, it is very well described and characterized. But the results are still inconclusive. However, based on the literature, it is highly likely that YL band is caused by a C-related defect.

CHAPTER 3

METHODOLOGY

3.1 Experimental technique

The spectra were investigated using steady-state photoluminescence and the time-resolved techniques.

Excitation of the steady-state PL was produced using He-Cd laser (30 mW, 325 nm). The PL produced by the sample was dispersed by the 1200 rules/mm grating in a 0.3 m monochromator and detected by the cooled photomultiplier detector. All the spectra were corrected with respect to system spectral responce.

For the time-resolved luminescence, a pulsed nitrogen laser was used. The laser excitation wavelength is 337 nm with pulse duration 1 ns and repetition rate 6 Hz. The response of the samples was analyzed using the above mentioned monochromator connected through the cooled photomultiplier detector to a digital oscilloscope.

Additional time-resolved PL study was carried out by Dr. Ümit Özgür, VCU. The nitrogen laser was used with 80 MHz repitition rate of 1ns wide pulses in temperature range from 15 K to 150 K.

3.2 Samples

The samples of GaN were provided by the Institute fur Experimentelle Physik, Otto-von-Guericke-Universitat Madelung, Magdeburg, Germany. These are the samples of GaN grown using MOCVD technique on (0001) sapphire substrates 0.25° off-oriented toward the m-direction. In [22] the ones were used to study the incorporation efficiency of carbon as an acceptor (series A), to achieve semi-insulating properties (series B) and to study the

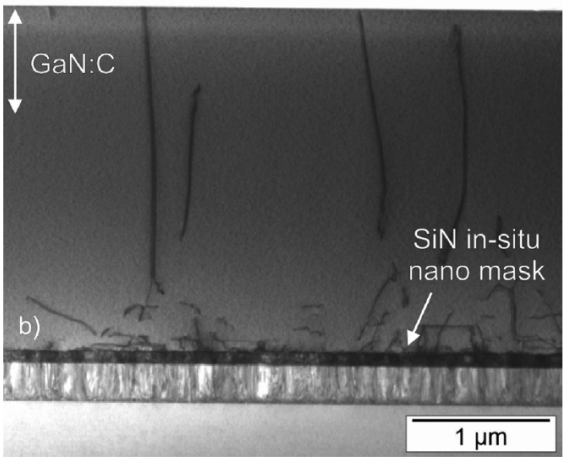

Fig. 10. STEM measurement of the sample C4 (adapted from [22])

impact on electrical leakage (series C). Series A and B were finalized by 650 nm sick Si, C co-doped GaN layer. Doping concentrations if Si and C were measured using second ion mass spectrometry (SIMS) and room-temperature Hall effect measurements corrected by size and location of the contacts. Moreover, scanning transmission electron microscopy (STEM) measurements in bright field contrast conditions were performed (Figure 10) in order to control the dislocation distribution on the carbon-doped layer of GaN. The parameters of the samples are given in Table 1. In this table each sample is numbered in the first column while in letters in the second column indicate to which series a particluar sample belongs. Next column is the quantum efficiency of the YL band measured at 300 K. The values of quantum efficiencies are normalized with respect to calibrated sample. Column four represents lifetime of the YL band in different samples at 300 K. The columns five and eight contain values of electron concentrations measured by PL and Hall effect. Finally columns six and seven give information about the concentrations of C and Si respectively.

Table 1. Parameters of the samples under the experiment

Sample No.	Series	η_{YL} (%) at 300 K	τ , (μs)at 300 K	n_{PL},(cm^{-3})	[C], (cm^{-3})	[Si], (cm^{-3})	n_{Hall},(cm^{-3})
9833	B	22	35	2.60E+17	6.00E+17	1.50E+18	9.70E+17
9834	A	6.3	0.9	1.01E+19	5.00E+17	6.00E+18	5.50E+18
9836	B	25	46	1.98E+17	6.00E+17	4.00E+17	semi-ins
9842	B	27	88	1.03E+17	7.00E+17	1.40E+18	7.50E+17
9843	B	26	110	8.26E+16	7.00E+17	1.00E+18	5.40E+17
9845	A	9	1.8	5.05E+18	2.00E+18	6.00E+18	3.75E+18
9847	A	12	8	1.14E+18	4.30E+18	6.00E+18	1.90E+18
9849	A	16	55	1.65E+17	5.30E+18	7.50E+18	4.00E+17
9851	B	12	4	2.27E+18	6.00E+17	3.10E+18	2.60E+18
9854	C	6	nonexp		4.60E+18	-	semi-ins
9856	C	0.3	2000	4.55E+15	8.00E+17	-	semi-ins
9857	C				2.90E+18	-	semi-ins
9867		0.00085				-	semi-ins
9891	C	0.5	>1000		1.60E+18	-	semi-ins
10052		0.0025				-	semi-ins
10152					1.50E+19	-	semi-ins
10142		0.0035			1.20E+19	-	semi-ins
10146		0.17	nonexp		5.50E+18	-	semi-ins
10150		0.0385	100	9.09E+16	6.70E+18	-	semi-ins

CHAPTER 4

RESULTS

4.1 Yellow and blue luminescence in GaN grown by MOCVD and co-doped with C and Si

Let's start with considering low-temperature steady-state PL spectra of various samples presented in Table 1 to ensure reproducibility. In Figure 11, one can see the spectra of several n-type samples of GaN:C, Si, measured at 0.00012 W/cm^2 excitation intensity. No bands can be seen except for YL, UVL and excitonic peak with their respective phonon replicas. The spectrum of the sample 9843 indicates the presence of C_NH or C_NO_NH complexes through BL2 band. In the samples 9847 and 9843, YL band is shifted significantly and the excitonic band is quite low. Exactly these samples were heavily doped with C and Si in similar quantities of $\sim 10^{18}$ cm^{-3}. In this case the dopants compensate each other almost exactly and their non-uniform distribution inside the sample cause fluctuations of the potential [23]. This affects the PL spectra by hifting bands to lower photon energies. With increasing excitation intensity, we observe an increase in the PL intensity of the excitonic peak and the decrease of YL. The most interesting effect occurs in-between the YL and UVL bands. The new BL_C band arises there (Figure 12), with properties, as will be shown below, very different from all the other bands known in GaN. In order to make the BL_C line more explicitly observable we focused excitation laser beam to concentrate photon density in a region of smaller area of the GaN:C, Si material.

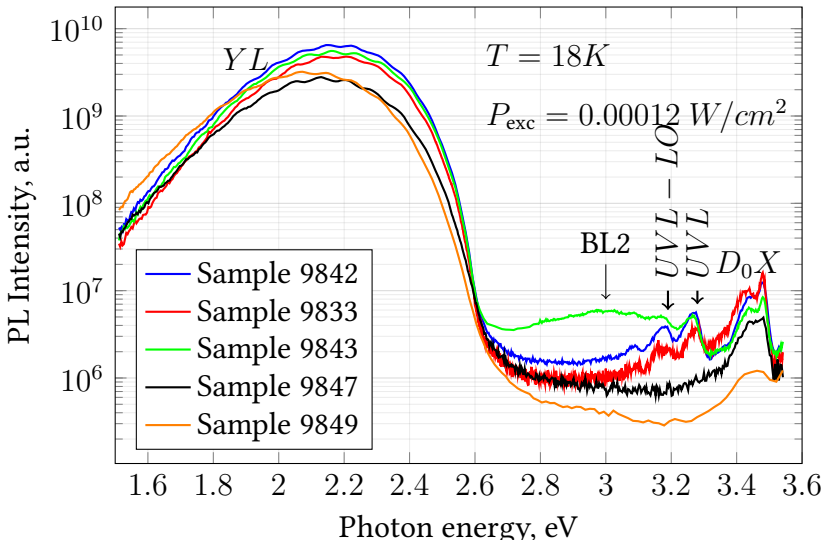

Fig. 11. Low-temperature spectra obtained at $P_{\text{exc}} = 0.00012$ W/cm^2 for various samples

4.1.1 Yellow luminescence band

The YL band has a maximum at 2.2 eV (Figure 14) along with ZPL at 2.59 eV and it begins to saturate at $P_{\text{exc}} > 10^{-1}$ W/cm^2. Since configuration coordinate model suits well for description of luminescence centers in crystals with strong electron-phonon coupling, the shape of the YL band, as well as many other bands, in the limit of low temperatures can be modeled as [20]

$$I_{\text{PL}}(\hbar\omega) = \exp\left\{-2S_e\left(\sqrt{\frac{E_0^* - \hbar\omega}{E_0^* - \hbar\omega_{\text{max}}}} - 1\right)^2\right\}, \tag{4.1}$$

where S_e is the Huang-Rhys factor, E_0^* is sum of the half dominant phonon energy for the excited state and the zero-phonon line energy, $\hbar\omega$ is the emitted photon energy. The YL band has exactly this shape $I_{PL}(\hbar\omega)$, which is steady for different excitation intensities, but the maximum position $\hbar\omega_{\text{max}}$ red-shifts from 2.2 eV by up to ~51 meV with decrease in excitation power density from 0.11 W/cm^2 to 0.12×10^{-3} W/cm^2. P_{exc}. This drift may be caused by weak fluctuations of potential. Indeed, at the locations of impurities the

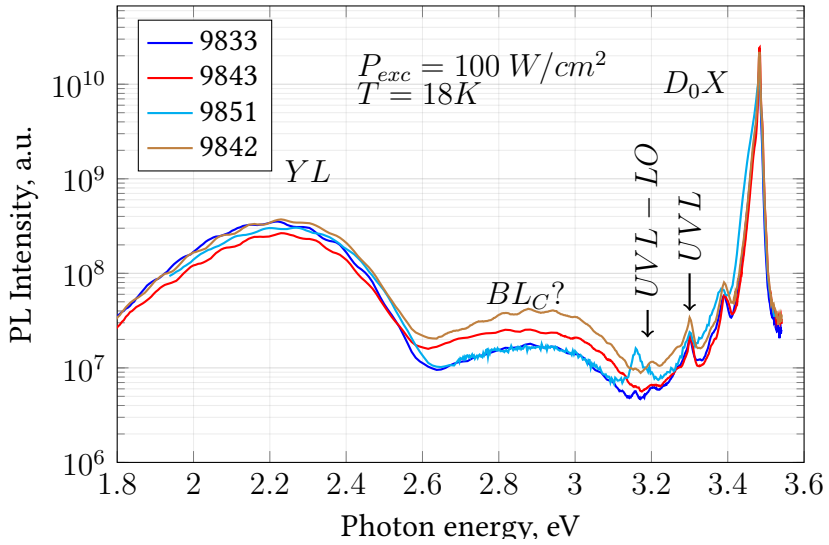

Fig. 12. Low-temperature spectra of the samples at high excitation intensities ($I_{\text{exc}} = 100\ W/cm^2$) with focused laser beam

valence and the conduction bands are deformed. In the case of high excitation intensity non-equilibrium carriers fill in the deformations flattening the potential landscape.

Excitation intensity influences YL significantly, and causes redistribution of the radiative recombination in favour of the other lines. Hence, with increase of excitaion intensity, the YL starts decreasing with simultaneous increase of intensities of BL_C, UVL and excitonic components of the spectrum. The set of corresponding spectra measured for the sample 9842 is depicted in Figure 14. BL_C band exhibits a significant enhancement with excitation power density.

4.1.2 Shape of the BL_C band

In the blue region of the PL spectra of GaN several bands can be found. BL1 band was extensively studied and was attributed to Zn substituting Ga point defect. This Zn-related PL band has the maximum at 2.90 eV [24]. Another blue band, named BL2, was observed in semi-insulating GaN samples and appears due to the presence of C_NH and C_NO_NH [25].

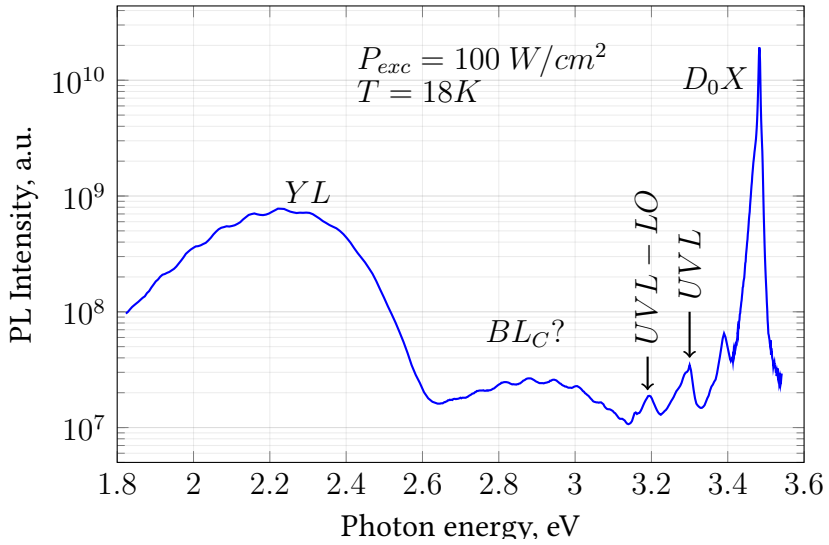

Fig. 13. Low temperature steady-state PL spectrum observed at excitation intensity $P_{\text{exc}} = 100W/cm^2$ under focused laser beam

Increase in excitation intensity P_{exc}, gives rise to a new line, that further will be called BL_C. It has a maximum at 2.87 eV and may be falsely identified as either BL1 or BL2.

However, our time-resolved PL measurements reveal that the BL_C band has an extremely fast decay about 1 ns, the corresponding decay is depicted in Figure 15. Time-resolved measurements at temperatures in the range from 15 to 150 K showed that the decay is independent of temperature. Hence, so does the electron-capture coefficient C_n of the respective recombination center. The corresponding lifetime for the BL_C is $\tau_{BL_C} \approx 1$ ns The BL_C band is unrelated to BL1, eventhough it has very close position of PL maximum. Indeed, it is known [26] that BL1 has lifetime of the order $\tau_{BL1} \approx 1\ \mu s$ but BL_C decays three orders of magnitude faster. This makes time-resolved PL a suitable technique for resolving these two bands.

The BL_C, cannot be related to BL2 either, since it is predicted [25] that the BL2 is caused by two possible complexes: C_NH or C_NO_NH with the maximum at 2.985 eV and its amplitude should decay upon long-time exposure to ultra-violet laser light [25]. Thus, the

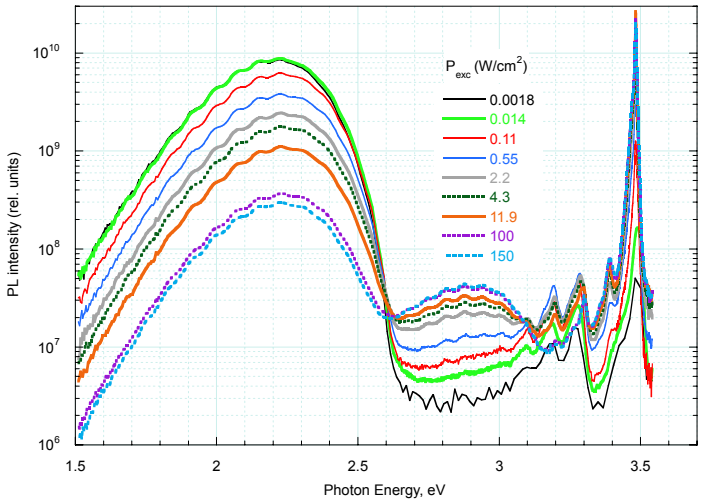

Fig. 14. Low temperature (T=14 K) spectra from n-type GaN excited by the focused laser beam

properties of the BL1 and BL2 bands are very different from the BL_C. Moreover, BL2 has been observed only in semi-insulating samples. The shape of the BL_C is hard to discern in steady-state PL since it has relatively low intensity and the significant overlap with YL and UVL bands. However, in time resolved PL it can be resolved relatively easy, due to the very short lifetime of BL_C. Figure 16 shows the shape of BL_C extracted using time-resolved PL by measuring the response of the sample to the 1 ns laser pulse excitation. The fitting was performed according to the formula (4.1) and resulted in the estimates of the following parameters: Huang-Rhys factor $S_e = 2.70$, band's maximum $\hbar\omega_{\max} = 2.87$ eV and $E_0^* = 3.20$ eV.

4.1.3 Excitation behavior

The dependence of PL intensities of the YL and BL_C bands on excitation intensity was obtained at T=150 K in order to avoid significant contribution from the tails of UVL and exciton bands. As it can be seen from Figure 17, decrease of the YL efficiency takes place when excitation P_{exc} increases. Simultaneously, it results in the steady increase in

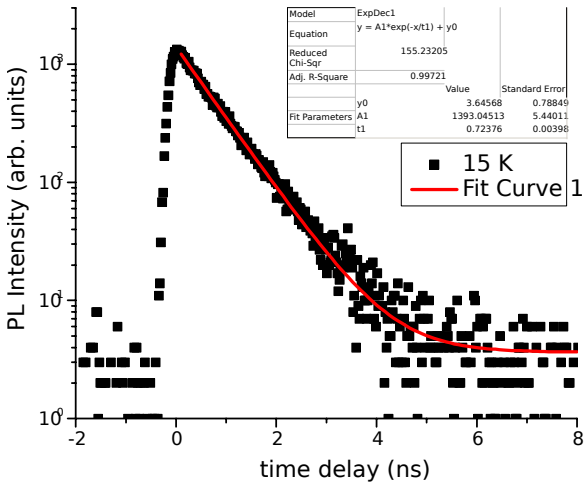

Fig. 15. Time decay of BL_C band at T=15 K and excitation intensity (Courtesy of Ümit Özgür, VCU)

PL intensity of BL_C. This bahvior can be explained by a redistribution of carriers between recombination channels. Since the (0/-) levels of C_N are filled by holes (when YL saturates), then the extra holes can be captured by the (0/+) level of C_N and produce BL_C.

The relation described in [27]

$$\frac{N_{A(YL)}}{N_{A(BL_c)}} = \frac{\eta_{YL}}{\eta_{BL_c}} \frac{C_{p(BL_c)}}{C_{p(YL)}} \tag{4.2}$$

can be used in our case to get the ratio of the hole-capture coefficients $C_{p(YL)}$ and $C_{p(BL_c)}$ of the states related to YL and BL_C bands respectively by determining the ratio of quantum efficiencies before saturation of the two bands η_{YL} and η_{BL_c}. Since, we assume that YL and BL_C are related to the same defect, then the right hand side of the above equation equals unity and we get

$$\frac{\eta_{YL}}{\eta_{BL_c}} = \frac{C_{p(YL)}}{C_{p(BL_c)}}. \tag{4.3}$$

In Figure 17, the dependence of the relative quantum efficiencies of YL and BL_C bands on the generation rate is shown. As it can be seen from Figure 14 at low excitation intensities BL_C cannot be distinguished from the background noise. Therefore, in Figure 17 BL_C

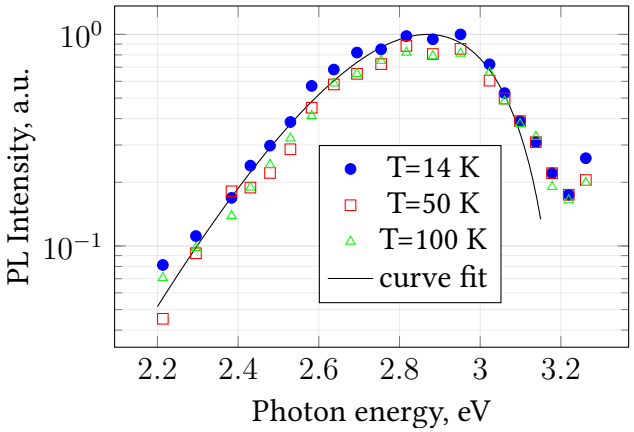

Fig. 16. Time-resolved BL_C band measured with 2 ns delay. The fitting was done using formula 4.1 with the parameters $S_e = 2.7$, $\hbar\omega_{\max} = 2.87$ eV and $E_0^* = 3.2$ eV.

dependence is distorted and the best we can infer from the graph is the lower bound for the above mentioned ratio of the hole-capture coefficients. Reading from the graph, we get the estimate $C_{p(YL)}/C_{p(BL_C)} \approx 300$. The hole-capture coefficient for the YL band is measured to be $C_{p(YL)} = 2 \times 10^{-7}\text{cm}^3/\text{s}$ [10], hence we can write an estimate for the $C_{p(BL_C)} \approx 7 \times 10^{-10}\text{cm}^3/\text{s}$.

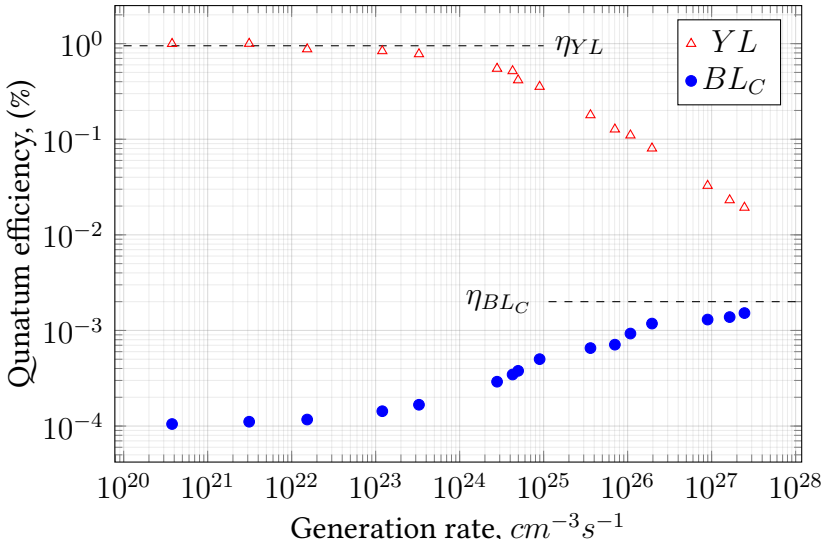

Fig. 17. Qunatum efficiency of YL and BL_C measured at T=150 K (sample 9842)

4.1.4 Temperature behavior

At high excitation intensity, the BL_C band is present in the spectrum up to at least 300 K, but around 120 K it starts quenching as well as accompanying YL band does (Figure 18). Both bands behave alike with temperature though YL significantly broadens

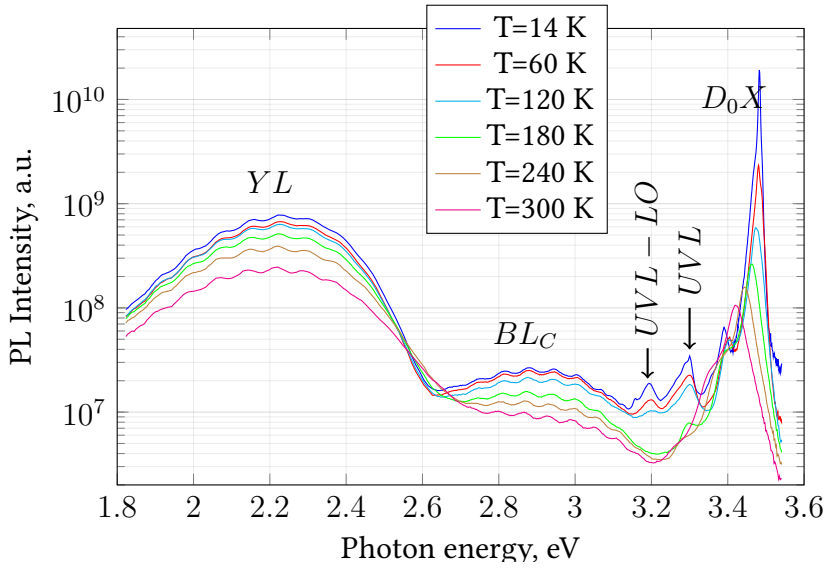

Fig. 18. Steady-state PL spectra at various temperatures under 100 W/cm^2 excitation intensity

admixing to the BL_C.

The temperature dependencies of quantum efficiencies of the YL and the near-band-edge (NBE) emission, obtained at low excitation intensities, are depcited in Figure 19. The YL band starts quenching at temperature around 400 K. The measurements of the YL intensity can be fitted with formula

$$I_{PL} = \frac{I_{PL}(0)}{1 + C\exp\left\{-\frac{E_A}{k_B T}\right\}} \tag{4.4}$$

that is just the simple consequence of (1.23). Along with the YL band, the temperature dependence of the NBE emission was plotted. One can see the rising step in the temperature

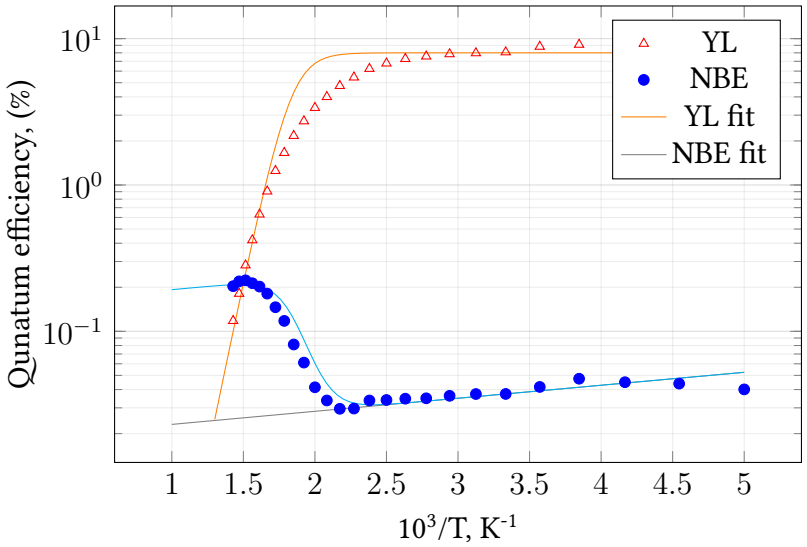

Fig. 19. Quantum efficiencies of the YL and NBE bands as functions of inverse temperature (sample 9842, $I_{\text{exc}} = 0.14W/cm^2$)

dependence of the NBE that starts growing when YL begin decreasing. Indeed, in general, thermal quenching of one channel results in redistribution of the released holes among all other radiative and non-radiative channels. That stepwise change in quantum efficiency by R_{NBE} can be used to determine internal quantum efficiency of the YL through the relation [28]

$$\eta_{YL} = \frac{R_{NBE} - 1}{R_{NBE}}. \tag{4.5}$$

Hence, for our case quantum efficiency of YL, given $R_{NBE} = 10$, $\eta_{YL} = 0.9$. The deviation of data from the fit in the bending region may be explained by weak potential fluctuations or surface effects such as band bending.

4.2 Discussion

Taking into account characteristics of the BL_C band, and its relation to the YL, we tend to attribute them to the two charge states of the C_N defect proposed in [14, 16].

One of the supporting arguments, though not very strong, is that the positions of the

YL and BL_C bands are in good agreement with the ones predicted. However, work still yet to be done to refine those calculations.

Also, BL_C has the smaller hole-capture coefficient compared to YL band. The reason for that may be thought in terms of the two charge states of C_N. When the acceptor catches a hole on (0/-) level, it becomes neutral. Hence, in this configuration, probability to catch another hole at (+/0) level should be lower because there is no Coulomb attraction. This matches our observations of the intensity of the BL_C band being much weaker than that of YL.

On the other hand , the radiative capture of the electrons is extremely fast ($\sim$ 1 ns) by the defect responsible for the BL_C. It is much faster (by a factor of 10^2-10^3) than the radiative capture of electrons by accpetors in GaN, such as Mg_{Ga} (UVL band), Zn_{Ga} (BL1 band), and the (0/-) level of C_N (YL band). This can be explained by Coulomb attraction of a free electron by the positively charged C_N^+ defect having two bound holes. Still, the possibility that the BL_C band is caused by a different defect cannot be excluded. In this case, we expect that it may be a donor with high electron-capture coefficient and low hole-capture coefficient. One of the candidates is the C_NSi_N [15].

CHAPTER 5

SUMMARY

In this work, the samples of GaN doped with C and Si were studied using steady-state and time-resolved photoluminescence technique. The samples were intentionally doped with C and Si in order to study the efficiency of incorporation of C and effects of compensation in GaN. The strongest PL band in these smples was the YL band with a maximum at ~ 2.2 eV. The quantum efficiency of this band approached 90% in some samples.

Steady-state PL measurements with high excitation intensity pointed out at the presence of the new PL band, named BL_{C}, with a maximum at about 2.9 eV. The band turned out to be completely different from the BL1 and BL2 bands, previously attributed to Zn_{Ga} and C_NH (or C_NO_NH) complexes, respectively. The BL_C has at least three orders of magnitude shorter decay time then that of BL1 and BL2. That makes time-resolved PL measurements the most suitable to observe it and infer parameters. The BL_C persists up to room temperature unlike BL2 that disappears at temperatures around 150 K. Moreover, BL_C is not subjected to bleaching under long-term UV exposure, that allows it to be relatively easy discerned from the BL2.

The BL_C band has an extremely short decay time $\tau \approx 1.0\, ns$. This decay time does not change from 15 K and 150 K. Hence, the electron capture coefficients of the corresponding state are steady in the same temperature range. Comparison of relative quantum efficiencies of YL and BL_C yielded lower bound for the ratio of hole-capture coefficients $C_{p(YL)}$ and $C_{p(BL_{\mathrm{C}})}$ to be at least 300.

Since there is a strong overlap of the BL_C with the YL and UVL bands, as well as with the tail of excitonic peak, we used time-resolved PL in order to determine the shape

of the BL_C. The shape can be closely approximated by the simple formula (4.1), derived from one-dimensional configuration coordinate model. The ZPL for the BL_C band was roughly estimated as 3.2 eV from the shape of the band. Maximum of the band lies at 2.87 eV, Huang-Rhys factor S_e, estimated from the same fit, is about $S_e = 2.7$, indicating moderate electron-phonon coupling for the defect.

The new BL_C band is attributed to the second charge state of the C_N defect. According to first-principle calculations, the C_N defect has two transition levels: (0/-) and (+/0) predicted to be at 0.9 eV and 0.35 eV above the valence band respectively. The maxima of the corresponding lines are predicted at 2.14 eV and 2.70 eV and their ZPLs are expected at 2.60 eV and 3.15 eV, respectively. The discrepancies between theory and experiment can be partly attributed to the high level of dopants in the samples causing fluctuations of the potential, that slightly shifts bands especially subjected to the various levels of excitation.

Appendix A

ABBREVIATIONS

PL	photoluminescence
GaN	gallium nitride
DFT	density functional theory
ZPL	zero-phonon line
MOCVD	metal-organic chemical vapour deposition
NBE	near-band-edge
YL	yellow luminescence
UVL	ultraviolet luminescence
BL	blue luminescence

REFERENCES

[1] Hadis Morkoç. *Handbook of nitride semiconductors and devices, Materials Properties, Physics and Growth*. Vol. 1. John Wiley & Sons, 2009.

[2] Hiroshi Amano et al. "P-type conduction in Mg-doped GaN treated with low-energy electron beam irradiation (LEEBI)". In: *Japanese Journal of Applied Physics* 28.12A (1989), p. L2112.

[3] Shinji Terao et al. "Fracture of AlxGa1-xN/GaN Heterostructure–Compositional and Impurity Dependence–". In: *Japanese Journal of Applied Physics* 40.3A (2001), p. L195.

[4] We Shockley and WT Read Jr. "Statistics of the recombinations of holes and electrons". In: *Physical review* 87.5 (1952), p. 835.

[5] Re N Hall. "Electron-hole recombination in germanium". In: *Physical review* 87.2 (1952), p. 387.

[6] Minko Balkanski and Richard Fisher Wallis. *Semiconductor physics and applications*. Vol. 8. Oxford University Press, 2000.

[7] Lev Davidovich Landau and Evgenii Mikhailovich Lifshitz. *Quantum mechanics: non-relativistic theory: V. 3: Course of Theoretical Physics*. Pergamon Press, 1958.

[8] Ivan Pelant and Jan Valenta. *Luminescence spectroscopy of semiconductors*. Oxford University Press, 2012.

[9] Jacques I Pankove. *Optical processes in semiconductors*. Courier Corporation, 1971.

[10] MA Reshchikov et al. "Thermal quenching of the yellow luminescence in GaN". In: *Journal of Applied Physics* 123.16 (2018), p. 161520.

[11] Toshio Ogino and Masaharu Aoki. “Mechanism of yellow luminescence in GaN”. In: *Japanese Journal of Applied Physics* 19.12 (1980), p. 2395.

[12] Jörg Neugebauer and Chris G Van de Walle. “Gallium vacancies and the yellow luminescence in GaN”. In: *Applied Physics Letters* 69.4 (1996), pp. 503–505.

[13] J. L. Lyons, A. Janotti, and C. G. Van de Walle. “Carbon impurities and the yellow luminescence in GaN”. In: *Applied Physics Letters* 97.15 (2010), p. 152108.

[14] Denis O. Demchenko, Ibrahim C. Diallo, and Michael A. Reshchikov. “Yellow luminescence of gallium nitride generated by carbon defect complexes”. In: *Physical review letters* 110.8 (2013), p. 087404.

[15] Sayre G Christenson et al. “Carbon as a source for yellow luminescence in GaN: Isolated CN defect or its complexes”. In: *Journal of Applied Physics* 118.13 (2015), p. 135708.

[16] J. L. Lyons, A. Janotti, and C. G. Van de Walle. “Effects of carbon on the electrical and optical properties of InN, GaN, and AlN”. In: *Physical Review B* 89.3 (2014), p. 035204.

[17] C. H. Seager et al. “Role of carbon in GaN”. In: *Journal of applied physics* 92.11 (2002), pp. 6553–6560.

[18] C.H. Seager et al. “Luminescence in GaN co-doped with carbon and silicon”. In: *Journal of Luminescence* 106.2 (2004), pp. 115–124. ISSN: 0022-2313.

[19] R. Armitage, Q. Yang, and E. R. Weber. “Analysis of the carbon-related blue luminescence in GaN”. In: *Journal of applied physics* 97.7 (2005), p. 073524.

[20] Michael A Reshchikov et al. “Carbon defects as sources of the green and yellow luminescence bands in undoped GaN”. In: *Physical Review B* 90.23 (2014), p. 235203.

[21] MA Reshchikov et al. “Zero-phonon line and fine structure of the yellow luminescence band in GaN”. In: *Physical Review B* 94.3 (2016), p. 035201.

[22] Andreas Lesnik et al. “Properties of C-doped GaN”. In: *physica status solidi (b)* 254.8 (2017).

[23] Boris Isaakovich Shklovskii and Alex L Efros. *Electronic properties of doped semiconductors*. Vol. 45. Springer Science & Business Media, 2013.

[24] MA Reshchikov et al. “Determination of the electron-capture coefficients and the concentration of free electrons in GaN from time-resolved photoluminescence”. In: *Scientific reports* 6 (2016), p. 37511.

[25] DO Demchenko, IC Diallo, and MA Reshchikov. “Hydrogen-carbon complexes and the blue luminescence band in GaN”. In: *Journal of Applied Physics* 119.3 (2016), p. 035702.

[26] Michael A Reshchikov. “Time-resolved photoluminescence from defects in n-type GaN”. In: *Journal of Applied Physics* 115.10 (2014), p. 103503.

[27] Michael A Reshchikov and Hadis Morkoc. “Luminescence properties of defects in GaN”. In: *Journal of applied physics* 97.6 (2005), pp. 5–19.

[28] Michael A Reshchikov et al. “Tunable and abrupt thermal quenching of photoluminescence in high-resistivity Zn-doped GaN”. In: *Physical Review B* 84.7 (2011), p. 075212.

VITA

Mykhailo Vorobiov was born on December 18, 1990, in Kharkiv, Ukraine and holds Ukrainian citizenship. He received his Bachelor and Master degrees in electrical engineering from Kharkiv National University of Radioelectronics, Kharkiv, Ukraine in 2012 and 2013 respectively. Subsequently he worked as a signal processing engineer and machine learning engineer for three years before joining the Department of Physics at VCU.